RESEARCH ARTICLE | JULY 22 2024

Solid waste slurry grouting transformation mechanism of loose sand layer based on slurry-water replacement effect

Xianxiang Zhu ; Qi Zhang ; Wenquan Zhang ; Lei Jin ; Zixu Li

Physics of Fluids 36, 073330 (2024)
https://doi.org/10.1063/5.0217551

Physics of Fluids ARTICLE pubs.aip.org/aip/pof

Solid waste slurry grouting transformation mechanism of loose sand layer based on slurry-water replacement effect

Cite as: Phys. Fluids **36**, 073330 (2024); doi: 10.1063/5.0217551
Submitted: 5 May 2024 · Accepted: 1 July 2024 ·
Published Online: 22 July 2024

Xianxiang Zhu,[1,2] Qi Zhang,[3,a)] Wenquan Zhang,[1,2] Lei Jin,[2] and Zixu Li[1,2]

AFFILIATIONS

[1]College of Energy and Mining Engineering, Shandong University of Science and Technology, Qingdao 266590, China
[2]State Key Laboratory of Mining Disaster Prevention and Control Co-founded by Shandong Province and the Ministry of Science and Technology, Shandong University of Science and Technology, Qingdao 266590, China
[3]Department of Civil and Environmental Engineering, The Hong Kong Polytechnic University, Kowloon, HongKong 999077, China

[a)]**Author to whom correspondence should be addressed:** q7zhang@polyu.edu.hk

ABSTRACT

During coal mining, when loose water-bearing sand layers are exposed and connected, it is extremely easy to cause water and sand inrush accidents, threatening the lives and properties in mines. Because of the intricate and tortuous internal structure of the sand layer, the diffusion pattern of grouting slurry within the loose sand layer has not been accurately characterized. Improving the efficiency of grouting and reducing the cost of grouting are common difficulties faced by industrial and mining enterprises in the grouting renovation of loose water-bearing sand layers. This paper innovatively proposes the mechanism of slurry-water displacement effect based on the diffusion characteristics of grouting slurry within the water-bearing sand layer. It studies the power-law fluid seepage and diffusion mechanism of porous media tortuosity effect and slurry-water displacement effect and derives the spherical diffusion equation of power-law fluid seepage grouting considering the coupling of porous media tortuosity effect and slurry-water displacement effect. At the same time, an indoor experimental device considering the slurry-water displacement effect is designed to verify the rationality of the spherical seepage grouting diffusion equation considering the superimposed effects of the two. Furthermore, relying on the COMSOL Multiphysics platform, a three-dimensional numerical calculation model of the power-law fluid spherical seepage grouting mechanism considering the porous media tortuosity effect and slurry-water displacement effect is constructed. It analyzes the seepage and diffusion characteristics of power-law grouting slurry in water-bearing sand layers, and studies the influence of different porosity of loose water-bearing sand layers, spacing between slurry and water holes, grouting pressure, and slurry viscosity on the volume of loose water-bearing sand layers. The key factors affecting the volume of loose water-bearing sand layers are grouting pressure > spacing between slurry and water holes > porosity of sand layer > slurry viscosity. Compared with previous grouting technologies and processes, the slurry-water displacement grouting technology can solve the problems of small grouting diffusion range and poor grouting effect in high-pressure underwater water-bearing sand layers to a certain extent.

I. INTRODUCTION

Currently, the shallow-buried coal reserves in the northern region of Anhui and the western area of Shandong, China, have entered the late stages of extraction. The future recoverable coal resources in these regions are characterized by deep burial, thick unconsolidated layers, and high water pressure. The coal reserves that can be extracted under these geological conditions exceed 150×10^6 tons (Song *et al.*, 2018; Ma *et al.*, 2021). Due to the poor mechanical properties and high water content of the sand layers, which exhibit favorable flow characteristics, they are prone to the formation of weak links under construction disturbance and underground water action. Once these weak links are disrupted, the development of water-bearing fractures and weak structural planes may escalate into water inrush and sand burst incidents, posing a significant threat to underground safety and production (Li *et al.*, 2020; Kalore and Babu, 2020). With the comprehensive economic recovery, the energy industry is at the forefront of the economic development of various nations. This makes it imperative to urgently extract the coal resources in the western part of Shandong and the northern part of Anhui. Addressing the key issue of improving the mechanical properties of water-containing loose sand layers and

reducing the probability of water inrush and sand bursts in these layers is crucial for the future safety of coal mining operations.

Experts and scholars both domestically and internationally have conducted extensive research on the extraction of coal seams beneath thick unconsolidated layers and extremely thick unconsolidated layers (Yu *et al.*, 2020; Zhang *et al.*, 2022). Taking a coal mine in the Lunan mining area as an example, Liu *et al.* (2023) explored the variation patterns of surface deformation parameters during coal seam extraction under different thickness ratios of unconsolidated layers to bedrock. Based on field measurements, the study analyzed surface deformation characteristics and assessed the impact of the loose-to-bedrock ratio on probability integration method parameters. Peng *et al.* (2022) investigated the mechanism and characteristics of surface subsidence during coal seam extraction beneath thick unconsolidated layers with an underlying impermeable bedrock. The analysis of the water-soil coupling stress-deformation mechanism during the consolidation process revealed that the presence of impermeable consolidation at the bottom of thick unconsolidated layers led to settlement, increasing the subsidence in the basin, and slowing down the convergence rate at the basin's edges, significantly expanding both vertical and horizontal movements of the surface. Using rheology theory and probability integration method, Hou *et al.* (2018) developed a superimposed model for predicting dynamic settlement in mining areas with thick unconsolidated layers. The model's accuracy was validated by comparing it with actual deformation data from mines. Li *et al.* (2017) studied various factors related to water inrush accidents induced by coal seam extraction beneath thick unconsolidated layers and thin bedrock. The study concluded that extraction methods, extraction height, bedrock thickness, and water pressure are the primary factors influencing water inrush disasters in the roof of unconsolidated layers. Focusing on geological conditions in the Shendong mining area, particularly shallow coal seam depth, thin overlying bedrock, and thick unconsolidated water-bearing layers, Fang *et al.* (2016) conducted a study on the cutting area of the 12 207 working face at the Shangwan coal mine. The research predicted mine water inflow by studying the height of the caving zone, water-conducting fractures, and the height of coal and rock columns for water and sand prevention. Currently, most research focuses on problems related to water inrush and surface subsidence caused by thick unconsolidated layers and thin bedrock. There is relatively limited research on prevention and control measures before coal seam extraction beneath thick unconsolidated layers and thin bedrock.

Compared to other rock layers, loose water-bearing sand layers have a higher porosity, making them amenable to modification through permeation grouting (Fraccica *et al.*, 2022; Mollamahmutoglu and Yilmaz, 2011; and Zhang *et al.*, 2022). The theoretical and technical methods for permeation grouting are currently quite abundant. The spherical diffusion theory and cylindrical diffusion theory, established based on Darcy's law, have become the foundation for many scholars researching permeation grouting theory (Ye *et al.*, 2020; 2019). To address the short diffusion distance issue in on-site grouting, Huang *et al.* (2018) proposed the vacuum grouting method. By correcting the boundary conditions of the Maag spherical diffusion model using the distribution pattern of vacuum pressure, a corrected model for vacuum grouting was derived. Wang *et al.* (2023) studied the diffusion law of Newtonian fluid during the process of grouting with a tube. Based on fractal theory and considering the effects of porous media tortuosity and the variable viscosity of the slurry, a two-level cylindrical-hemispherical diffusion model for Newtonian fluids was derived. The study analyzed the impact of constant flow grouting on grout pressure and diffusion radius, considering the influences of grouting flow rate, slurry viscosity, and tortuosity on grouting pressure and diffusion radius under constant flow grouting. Using the capillary laminar flow model, Xie *et al.* (2022) derived the equation for the percolation movement of power-law fluids. By considering the effects of tortuosity and the variable viscosity of the slurry in porous media, a grouting method that considers both tortuosity and the variable viscosity of the slurry was established and validated through existing experiments. Guo *et al.* (2021), in considering the variable viscosity of power-law slurry, and Yang *et al.* (2021), in studying the mechanism of cylindrical permeation grouting considering tortuosity, both developed three-dimensional permeation grouting spherical diffusion numerical models based on the COMSOL numerical simulation platform. By comparing the numerical simulation results with and without considering diffusion paths, the necessity of considering diffusion paths was demonstrated. Currently, there is abundant research on the reinforcement of surface-buried sand layers using permeation grouting theory in fields such as tunnel excavation and coastal infrastructure. However, there is still limited research on the permeation grouting mechanism of power-law fluids in loose water-bearing layers underground, and there is no method for determining the direction of grouting, which makes it challenging to guide current engineering practices.

This study based on the geological conditions of a mine in the Heze mining area with thick loose water-bearing sand layers, proposes a slurry-water replacement mechanism that ensures safety while maximizing coal recovery. Using Darcy's law and the law of mass conservation, we establish a power-law fluid permeation grouting spherical diffusion mechanism considering the tortuosity effect of loose water-bearing sand layers and the slurry-water replacement effect. We use self-developed laboratory equipment to validate theoretical equations. Through the coupling of theoretical equations in the COMSOL numerical simulation software, we develop a three-dimensional numerical model for power-law fluid grouting spherical diffusion that considers the tortuosity effect and slurry-water replacement effect. The study analyzes the impact of loose water-bearing sand layer properties and slurry properties on the volume of the loose water-bearing sand layer and identifies key factors affecting slurry diffusion. Compared to previous grouting technologies and processes, slurry-water replacement grouting technology can, to a certain extent, address issues such as small grouting diffusion range and poor grouting effects in water-bearing layers under high-pressure conditions.

II. SLURRY-WATER REPLACEMENT MECHANISMS IN LOOSE WATER-BEARING SAND LAYERS

The inherent properties of the sandy soil layer determine the feasibility of slurry permeation grouting, while factors such as the maximum particle size, self-stability, and fluidity of the slurry determine its injectability and applicability. The slurry can only be injectable when the particle size in the slurry is smaller than the minimum pore size of the sandy soil layer (Han *et al.*, 2022).

Loose water-bearing sand layers act as porous media where water plays a role in filling voids and sharing the seepage pressure (Zhang *et al.*, 2024a; 2023b). Simply installing grouting pipes in the loose water-bearing sand layer causes the slurry, under grouting pressure, to enter the sand layer, compressing the sand around the grouting pipe, making the sand layer's pores compact, and limiting the diffusion

range of the slurry. This results in a small reinforcement area, increases the borehole rate for the target layer, raises production costs, and, given the good fluidity of loose water-bearing sand layers, can lead to widespread collapse holes and hazards like water inrush and sand bursts (Wang *et al.*, 2023). Therefore, it is advisable to consider installing drainage holes at certain intervals while grouting. Creating a pressure difference between the grouting area and drainage holes induces a flow path from the grouting hole to the drainage hole due to the inherent fluidity of water in the aquifer. This allows water to flow out, slurry to fill the voids in the sand layer, and the consolidation of the sand layer. This displacement process transforms the loose water-bearing sand layer, reducing the probability of water inrush and sand bursts Dong *et al.*, 2022).

During the consolidation process of permeation grouting in loose water-bearing sand layers, grouting holes and drainage holes are alternately arranged. Applying drainage pressure during grouting creates a pressure difference within the water-bearing sand layer. The slurry, in fluid form, flows from high-pressure areas to low-pressure areas. Continuous drainage pressure induces the flow of slurry toward the drainage holes, facilitating extensive diffusion and permeation of the slurry within the internal sand body. This achieves the transformation of the target layer, as illustrated in Fig. 1.

III. POWER-LAW FLUID SPHERICAL INFILTRATION GROUTING THEORY CONSIDERING TORTUOSITY EFFECT AND SLURRY-WATER REPLACEMENT IN POROUS MEDIA

A. Basic assumptions

(1) The water-rich sand layer is homogeneous and isotropic, experiencing no deformation during the grouting process.
(2) Fill-pressure densification grouting is employed, with the slurry injected only from the bottom of the grouting pipe.
(3) The interior of the water-rich sand layer is a closed space, uniformly distributed, and does not consider gas-liquid displacement.
(4) Flow-solid coupling effects are not considered, and chemical reactions of the slurry are omitted.
(5) The slurry is a power-law fluid, exhibiting spherical diffusion in the geological formation, and the seepage diffusion process is laminar.

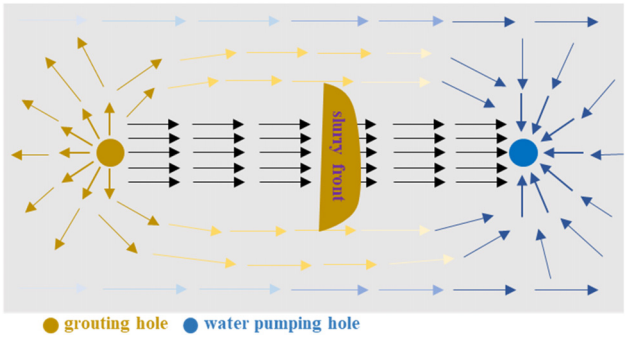

FIG. 1. Schematic diagram of slurry-water replacement effect in water-rich sand layer.

B. Power-law fluid osmotic diffusion mechanism considering porous medium tortuosity effect and slurry-water displacement effect

1. Rheological equations for power-law fluids

The rheological equation (Pantokratoras, 2016) for a power-law fluid is

$$\tau = c\gamma^n, \tag{1}$$

$$\gamma = -\frac{dv}{dr}, \tag{2}$$

where τ is the shear stress, MPa; n is the power law index; c is the power law coefficient; γ is the shear rate, m/s; v is the seepage velocity of the power law fluid in the porous medium, m/s; and r is the diffusion radius of the power law fluid in the porous medium.

2. Power-law fluid seepage motion equation considering porous media tortuosity and slurry-water replacement effect

The actual flow of fluid in the sand layer does not follow the theoretical calculated diffusion; instead, it exhibits a convoluted and tortuous diffusion based on the pore conditions within the sand layer, showcasing typical tortuosity effects (Civan, 2010), as illustrated in Fig. 2.

Currently, based on the research findings of domestic and international experts and scholars, tortuosity is commonly employed to reflect the actual extent of fluid diffusion in porous media. Kong (1999) conducted a study on tortuosity in porous media and found that the distribution of tortuosity in porous media typically falls within the range of 2.00–2.50. The formula for tortuosity is as follows:

$$\xi = \left(\frac{L_e}{L}\right)^2. \tag{3}$$

In the equation, L_e represents the actual flow path length of the fluid in porous media, L is the theoretical length of fluid in porous media, and ζ denotes the tortuosity of the porous media.

In the initial grouting state of porous media, the pore water pressure in the sand layer around the grouting hole is approximately equal. If drainage holes are arranged at intervals around the grouting hole and drainage pressure is applied simultaneously, creating a negative

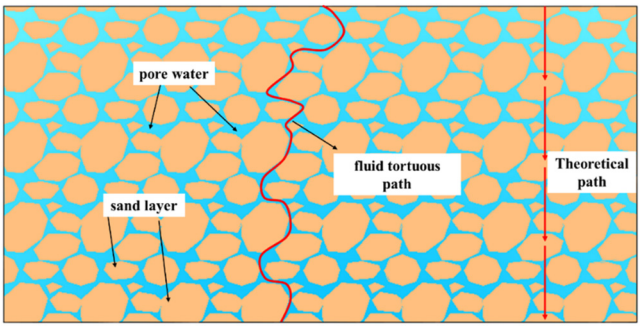

FIG. 2. Schematic diagram of the actual diffusion of a power-law fluid in a porous medium.

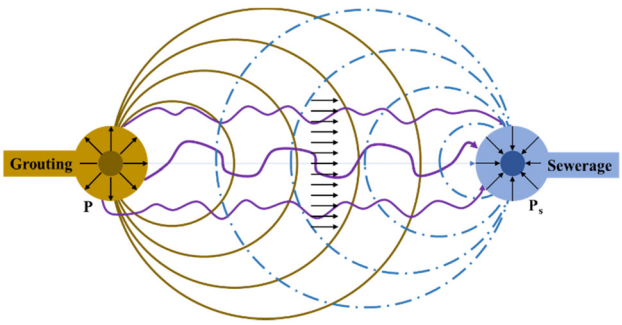

FIG. 3. Pressure field distribution of grouted seepage in porous media with slurry-water replacement effect.

pressure zone between the grouting hole and the drainage hole, the pressure difference will cause the slurry to transfer toward the drainage hole area, as illustrated in Fig. 3. The seepage pressure between the grouting hole and the drainage hole is composed of the grouting pressure and drainage pressure.

In Fig. 3, the actual diffusion of the power-law fluid due to the tortuosity effect is illustrated. We select a micro-flow unit for analysis, as shown in Fig. 4. The left side has a pressure of grouting pressure P, P_w is the groundwater pressure, and r_s is the radius of the drainage hole. The right side has a pressure of $P + dP + P_s - P_w$.

For a saturated and pressurized water-bearing sand layer subjected to drainage pressure, water flows toward the drainage hole in a spherical and centripetal manner. The seepage motion of water in the sand layer follows Darcy's law, where K_s is the permeability coefficient of water in the sand layer, and μ_s is the viscosity of water. Therefore

$$\frac{dp_s}{dr_s} = -\frac{\mu_s}{K_s} \cdot \frac{Q}{2\pi r_s^2}, \tag{4}$$

where r_w is the distance from the drain hole to any point in the flow field sphere. Integrating the above equation yields

$$p_s = p_w + \frac{Q_s \mu_s}{2\pi K_s}\left(\frac{1}{r_s} - \frac{1}{r_w}\right), \tag{5}$$

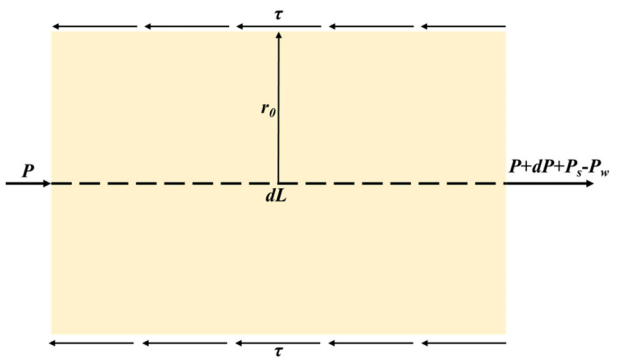

FIG. 4. Flow in porous media with power-law slurry units based on slurry-water replacement.

$$p_s - p_w = \frac{Q_s \mu_s}{2\pi K_s}\left(\frac{1}{r_s} - \frac{1}{r_w}\right). \tag{6}$$

Since in practice r_w is much larger than r_s

$$p_s - p_w = \frac{Q_s \mu_s}{2\pi K_s r_s}. \tag{7}$$

Under the condition of considering only the grouting pressure and seepage pressure, the force relationship of this microfluidic unit column in the pore space of the porous medium is

$$\pi r^2 (dp + P_s - P_w) + 2\pi r \tau dL = 0. \tag{8}$$

From this, it follows

$$r = -\frac{r}{2} \cdot \frac{dp + P_s - P_w}{dL}. \tag{9}$$

At the initial boundary where $r = r_0$ and $v = 0$, by combining Eqs. (1), (7), and (9) and employing the method of separation of variables, the seepage equation for power-law fluid in porous media can be obtained,

$$v = \frac{n}{n+1}\left(-\frac{1}{2c}\frac{dp + P_s - P_w}{dL}\right)^{\frac{1}{n}}\left(r_0^{\frac{n+1}{n}} - r^{\frac{n+1}{n}}\right). \tag{10}$$

The unit flow rate Q_d of a power-law fluid in a porous medium is given by

$$Q_d = \int_0^{r_0} 2\pi r v dr. \tag{11}$$

Substituting Eq. (10) into Eq. (11) and integrating give

$$Q_d = \frac{\pi n}{3n+1}\left(-\frac{1}{2c}\frac{dp + p_s - P_w}{dL}\right)^{\frac{1}{n}} \cdot r_0^{\frac{3n+1}{n}}. \tag{12}$$

Therefore, the average flow rate of a power-law fluid in a porous medium is

$$\bar{v} = Q_d = \frac{n}{3n+1}\left(-\frac{1}{2c}\frac{dp + p_s - P_w}{dL}\right)^{\frac{1}{n}} \cdot r_0^{\frac{n+1}{n}}. \tag{13}$$

Based on the study by Yang *et al.* (2005), by combining Eqs. (5), (7), and (11), the diffusion equation for seepage of power-law fluid in porous media considering tortuosity and slurry-water replacement effects can be derived,

$$V = \frac{\varepsilon_p n}{3n+1}\left(\frac{1}{2\sqrt{\xi}c}\right)^{\frac{1}{n}}\left(\frac{8\mu K}{\varepsilon_p}\right)^{\frac{n+1}{2n}}\left(-\frac{dp}{dL} - \frac{Q_s \mu_s}{2\pi K_s r_s dL}\right)^{\frac{1}{n}}. \tag{14}$$

3. Spherical diffusion mechanism of power-law fluid considering tortuosity and slurry-water replacement effects in porous media

Building upon the aforementioned assumptions and considering the tortuosity and slurry-water replacement effects in porous media, the spherical seepage diffusion mechanism of power-law fluid in porous media is depicted in Fig. 5. Here, r_0 represents the radius of the grouting hole, and r_1 is the final diffusion radius after time t.

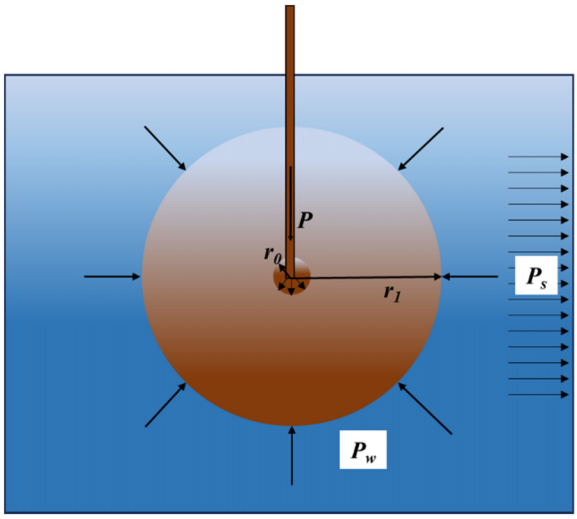

FIG. 5. Theoretical model of spherical diffusion of power-law fluid.

During the grouting process, the grouting volume is always satisfied according to the mass conservation equation,

$$Q = V\dot{A}t, \tag{15}$$

where A is any spherical surface of the slurry at moment t, which can be expressed as

$$A = 4\pi r^2. \tag{16}$$

This can be obtained by combining Eqs. (14)–(16) and solving

$$dp = -2\sqrt{\varepsilon}c \cdot \left(\frac{(3n+1)Q}{4\pi t\varepsilon_p n}\right)^n \cdot \left(\frac{\varepsilon_p}{8\mu K}\right)^{\frac{n+1}{2}} \cdot r^{-2n}dL - \frac{Q_s\mu_s}{2\pi K_s r_s}. \tag{17}$$

The solution of Eq. (17) can be obtained by using the separated variable integration method according to the boundary conditions of the spherical diffusion theory model in Fig. 5,

$$\Delta p = -2\sqrt{\varepsilon}c \cdot \left(\frac{(3n+1)Q}{4\pi t\varepsilon_p n}\right)^n \cdot \left(\frac{\varepsilon_p}{8\mu K}\right)^{\frac{n+1}{2}} \cdot \frac{r_1^{1-2n} - r_0^{1-2n}}{1-2n} - \frac{Q_s\mu_s}{2\pi K_s r_s}. \tag{18}$$

When the time is t, the grouting volume Q is

$$Q = \frac{4}{3}\pi r^3 t\varepsilon_p. \tag{19}$$

The power-law fluid spherical infiltration grouting diffusion equation based on the porous medium tortuosity effect and slurry-water displacement effect is derived by bringing in Eq. (18),

$$\Delta p = \frac{2\sqrt{\varepsilon}c}{1-2n} \cdot \left(\frac{2n+1}{3n}\right)^n \cdot \left(\frac{\varepsilon_p}{8\mu K}\right)^{\frac{n+1}{2}} \cdot (r_1^{1-2n} - r_0^{1-2n})r_1^{3n} - \frac{Q_s\mu_s}{2\pi K_s r_s}. \tag{20}$$

C. Scope of application

The power-law fluid spherical permeation diffusion and grouting diffusion equation [Eq. (20)], considering the tortuosity and slurry-water replacement effects in porous media, is derived based on the assumption of laminar flow. Therefore, it is not applicable under turbulent flow conditions.

According to the research findings of Zeng (1981), the stability coefficient Z is commonly used to determine whether the permeation and diffusion process of power-law fluid in porous media is in a laminar or turbulent state. The Z value is derived from the theory of laminar stability, suggesting that the transition from laminar to turbulent flow does not occur simultaneously across the entire cross section of the pipe but initially starts in the layer with the maximum turbulence. When $Z > 808$, the permeation and diffusion process of power-law fluid in porous media is in a turbulent state, while when $Z < 808$, it is in a laminar state.

The value of the stability factor Z is calculated using the following formula:

$$Z = \frac{n}{2^n}\left(\frac{1}{n+2}\right)^{\frac{n+2}{n+1}}\left(\frac{3n+1}{n}\right)^{2-n}\frac{d^v\bar{v}^{2-n}\rho}{c}, \tag{21}$$

where $\bar{v}$ is the average seepage velocity of power-law fluid in porous media, ρ is the density of slurry; and d is the pore scale of slurry permeation diffusion in porous media.

D. Verification analysis

To validate the accuracy of the spherical grouting diffusion equation for power-law fluid considering tortuosity and slurry-water replacement effects, this study will use a self-developed saturated water-bearing sand layer grouting simulation test device for verification.

1. Experimental setup

The grouting test device consists of four parts: pressure supply device, slurry storage tank, test box, and pumping device. The schematic diagram is shown in Fig. 6. The pressure supply device adopts a commonly used pressurized nitrogen cylinder on the market to provide pressure for grouting. At the same time, it can precisely control the pressure increase and decrease and the grouting time by adjusting the controller on the upper end of the nitrogen cylinder. The slurry storage tank is a device used to hold power-law fluids. By calculating the initial mass of the power-law fluid before and after grouting and the value of the flow meter during the grouting time, the mass of the power-law slurry injected into the porous medium can be obtained. The saturated water-bearing sand layer box is a cubic box composed of transparent acrylic plates, which is a device for completing the grouting test. The pumping device realizes slurry-water displacement by arranging drainage pipes in the saturated water-bearing sand layer and using a pump to drain the water in the saturated water-bearing sand layer while grouting starts, so that the pore water in the water-bearing sand layer is replaced by slurry. The physical diagram of the components of the test system is shown in Fig. 7.

2. Experimental materials

Based on the sampling results from the loose water-bearing sand layer on-site, without considering the repeatability and simplicity of the experimental process, saturated water-bearing sand layers were

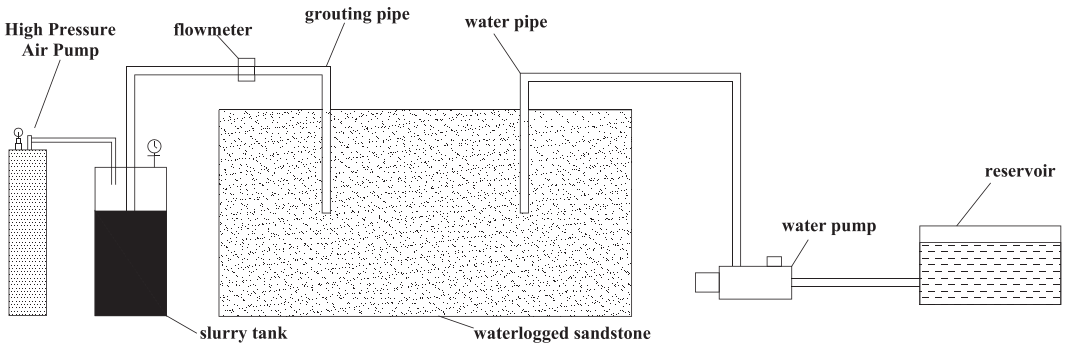

FIG. 6. Schematic diagram of the experimental setup for power-law fluid injection and diffusion experiment.

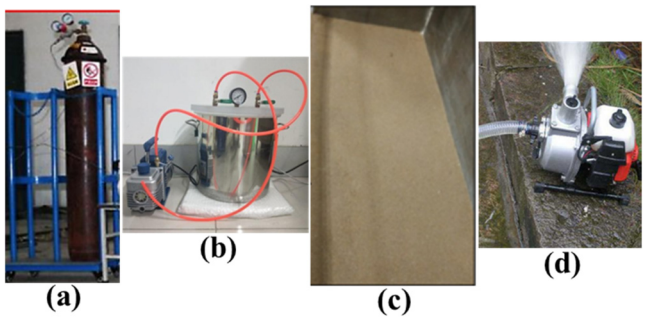

FIG. 7. Physical drawing of grouting test equipment: (a) Pressure supply unit; (b) slurry storage tank; (c) saturated water-bearing sand layer; and (d) suction pumps.

FIG. 8. Slurry injection of a crystalline body in a saturated sand layer: (a) Without considering slurry replacement and (b) considering slurry replacement.

created using river sand. The particle size distribution includes 30% for particles in the range of 0–0.25 mm, 55% for particles in the range of 0.25–0.5 mm, and 15% for particles in the range of 0.5–2 mm, as shown in Fig. 8. The porosity and permeability of the injected medium were determined separately through the "Soil Testing Methods Standard" and constant head permeability tests (GB/T50123, 2019). The permeability coefficient of the sand layer was measured to be 3.2 cm/s, with a porosity of 43%. To simulate the slurry-water replacement displacement effect in the saturated water-bearing sand layer under pressure, water needed to be injected into the model box before grouting to saturate the sand layer. The slurry used was a self-developed green grouting material (Zhu *et al.*, 2023), with a water-cement ratio of 0.7.

3. Control parameters

Constant-pressure grouting was adopted with design grouting pressures of 0.2, 0.4, and 0.6 MPa, drainage pressure of 0.2 MPa, static water pressure of 0.01 MPa, and grouting time controlled at 10 min. The spacing between grouting holes and drainage holes was set at 0.5 m.

4. Theoretical and experimental comparative analysis

To verify the correctness of the power-law slurry spherical permeation grouting diffusion equation considering tortuosity and slurry-water replacement effects, considering the time-variable viscosity of the slurry, the maximum diffusion radius [Eq. (20)] was compared with the experimental measured values under conditions of not considering tortuosity and slurry-water replacement effects, considering only tortuosity, considering only slurry-water replacement effects, and simultaneously considering tortuosity and slurry-water replacement effects. The theoretical values and measured values for each condition are presented in Table I, where L1, L2, L3, and L4 represent the theoretical values under conditions of not considering tortuosity and

TABLE I. Comparison of theoretical and measured values of slurry diffusion radius considering different influencing effects/mm.

Grouting pressure/MPa	T1	L1	Error (%)	L2	Error (%)	T2	L3	Error (%)	L4	Error (%)
0.2	86.4	152.4	43.31	116.4	25.77	127.8	187.6	26.55	154.6	10.87
0.4	161.3	234.8	31.30	183.9	12.29	214.6	268.4	20.04	233.3	8.02
0.6	208.9	286.4	27.06	223.4	6.49	289.3	384.5	18.39	312.6	7.45

slurry-water replacement effects, considering only tortuosity, considering only slurry-water replacement effects, and simultaneously considering tortuosity and slurry-water replacement effects, respectively. T1 represents the experimental process without considering slurry-water replacement effects, and T2 represents the experimental process considering slurry-water replacement effects.

From Fig. 9 and Table I, it can be concluded that for the same operating conditions, to enhance the maximum diffusion radius of the slurry in the saturated water-bearing sand layer, as the theoretical model is improved, the error between theoretical values and experimental values gradually decreases. When not considering the effects of porosity curvature and slurry-water displacement, the theoretical errors are the largest for each grouting pressure. When considering only the effect of porosity curvature, the relative error between the maximum slurry diffusion radius and the measured value decreases, indicating that the slurry's diffusion range in the porous medium is slowed down due to its viscosity and the porosity curvature effect. When considering only the slurry-water displacement effect, the promotion of drainage pressure creates a negative pressure zone within the range of grouting and drainage holes, enlarging the slurry diffusion range. However, without considering the curvature effect of the slurry in the porous medium, significant errors are still present. When simultaneously considering both the porosity curvature effect and the slurry-water displacement effect, the theoretical values, and experimental measurements for three grouting pressures are all within 20%, confirming the rationality of considering both porosity curvature and the variable viscosity of the slurry.

IV. NUMERICAL SIMULATIONS

The grouting process in the saturated confined aquifer sand layer is relatively concealed, and the diffusion mode of the slurry in this layer is mainly permeation. Currently, Darcy's law serves as the primary theoretical basis for addressing the seepage movement of slurry and water during the grouting process. Due to the complexity and high cost of the experimental process, the COMSOL Multiphysics numerical simulation software is utilized, based on computer programing techniques, to obtain a three-dimensional numerical simulation program through secondary development, which considers the tortuosity effect of the porous medium and the slurry-water displacement effect of the power-law fluid spherical permeation grouting mechanism [formula (20)]. This simulation program can not only achieve the numerical simulation of the spherical permeation and diffusion process of power-law fluid in porous media, but also ensure that the simulated permeation and diffusion process conforms to the theoretical basis of laminar flow state.

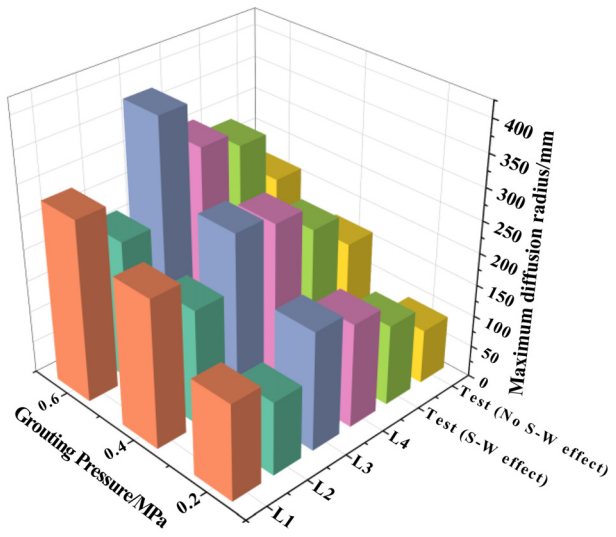

FIG. 9. Comparison of results between theoretical and experimental values.

A. Control equations

Building upon the assumptions made earlier, the fluid two-phase seepage theory is employed to describe the slurry diffusion process under static and dynamic water conditions. The control equations incorporate the time-variable viscosity function of the slurry and the actual curvature effects of the porous medium. Additionally, injection holes and drainage holes are introduced to facilitate the slurry-water displacement effect. The solution is obtained through the use of the two-phase Darcy law physical fields within the porous media and groundwater flow modules in COMSOL Multiphysics (Zhang *et al.*, 2023). The control equations employed are as follows:

Constant equation of continuity for water

$$-\left[\frac{\partial(\rho_o v_{ox})}{\partial x}+\frac{\partial(\rho_o v_{oy})}{\partial y}+\frac{\partial(\rho_o v_{oz})}{\partial z}\right]=\frac{\partial(\phi\rho_o S_o)}{\partial \tau}. \quad (22)$$

Constant equation of continuity of the slurry

$$-\left[\frac{\partial(\rho_w v_{wx})}{\partial x}+\frac{\partial(\rho_w v_{wy})}{\partial y}+\frac{\partial(\rho_w v_{wz})}{\partial z}\right]=\frac{\partial(\phi\rho_w S_w)}{\partial \tau}. \quad (23)$$

Controlled equations

$$S_o + S_w = 1, \quad (24)$$

where ρ_o is the density of the slurry; ρ_w is the density of water; φ is the porosity of the underlying sandstone; S_o is the volume fraction of the slurry in the pore space; S_w is the volume fraction of water in the pore space; and v is the seepage field velocity.

B. Parameter selection and model establishment

Based on the geological conditions of loose aquifer sand layers in Heze, China, referring to the physical test parameters of loose aquifer sand layers described by Zhang (2017), as well as the parameter measurement of power-law slurry by Zhu *et al.* (2023) in the earlier stage, as shown in Table II, the time-varying function of slurry viscosity is presented in Table III. A three-dimensional diffusion model for grouting in loose aquifer sand layers is established, considering the tortuosity

TABLE II. Analog parameter settings.

Slurry density/kg·m^{-3}	Slurry viscosity/Pa·s	Water density/kg·m^{-3}	Water viscosity/Pa·s
1600	0.012	1000	0.001

TABLE III. Time-varying functions of slurry viscosity.

Water-cement ratio	Aqueous form	Units
0.5	$70.2 \times 10^{-3} \times \exp(0.008\,74 \times t)$	Pa·s
0.6	$36.53 \times 10^{-3} \times \exp(0.0151 \times t)$	
0.7	$19.67 \times 10^{-3} \times \exp(0.0178 \times t)$	

effect of porous media and slurry-water displacement effect. The model dimensions are 4 m × 2 m × 2 m, with the grouting pipe and drainage pipe horizontally arranged in the middle, 1 m away from the left boundary, and the drainage pipe 1 m away from the right boundary. The distance between the two is 2 m. Both pipes have a length of 0.8 m and a radius of 0.05 m. The model is a closed space, and the outer walls are set as impermeable zero-pressure boundaries. The sand layer is initially set as a water storage model with an initial pore water pressure of 0.1 MPa and a constant pumping pressure of 2 MPa. The initial porosity of the sand layer is set to 0.43, and the permeability is 3.2×10^{-9} m^2. As the model is set in a closed space with minimal sand particle migration space, this paper does not consider the migration of sand particles carried by slurry, only focusing on the diffusion of slurry. The fluid diffusion coefficient model selects the Millington Quirk model embedded in COMSOL, and the fluid diffusion coefficient is set to 1×10^{-5} m^2/s. The initial grouting pressure is set to 4 MPa. The grid is divided into tetrahedral elements, including 187 009 domain elements, 11 330 boundary elements, and 764 edge elements. The model establishment and grid division are shown in Fig. 10.

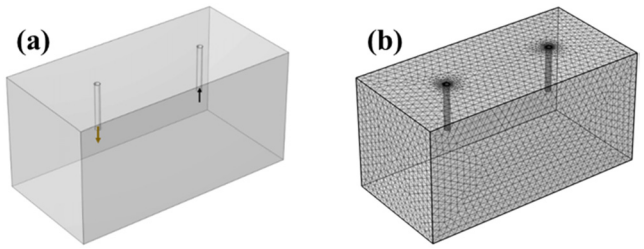

FIG. 10. Numerical modeling and meshing: (a) Establishment of three-dimensional numerical models and (b) mesh delineation.

C. Numerical simulation analysis

1. Characteristics of grout penetration and diffusion in water-bearing sand layer

Taking an example with an injection time of 1500 s, water-cement ratio of 0.5, and a spacing of 2 m between injection holes, and an injection pressure of 4 MPa, typical water-bearing sand layers were simulated. The above parameters were used to analyze the diffusion pattern of the slurry in the water-bearing sand layer, as shown in Figs. 11 and 12.

The numerical simulation results based on the above parameters are shown in Figs. 11 and 12. The diffusion range with slurry saturation of 0.5 and above is considered effective grouting. Therefore, the diffusion range with slurry saturation of 0.5–1.0 is taken as the effective range of permeation grouting, representing the effective volume range for reinforcing the sand layer. From the figures, it can be observed that the slurry undergoes spherical diffusion in the water-bearing sand layer, with or without slurry-water displacement effects, consistent with the theoretical derivation of the power-law fluid permeation grouting in loose water-bearing sand layers. Furthermore, when a drainage pipe is set to provide pumping pressure, the maximum diffusion radius of the slurry is 1.15 m. Without setting pumping pressure, the maximum diffusion radius is 0.75 m. The maximum diffusion radius of the slurry is increased by approximately 53.3% compared to the case without pumping pressure. The slurry diffuses along the negative-pressure zone toward the drainage hole area, exhibiting directional guidance. This displacement replaces the pore water in the target area, filling the pores in the sand layer, thereby reinforcing the target

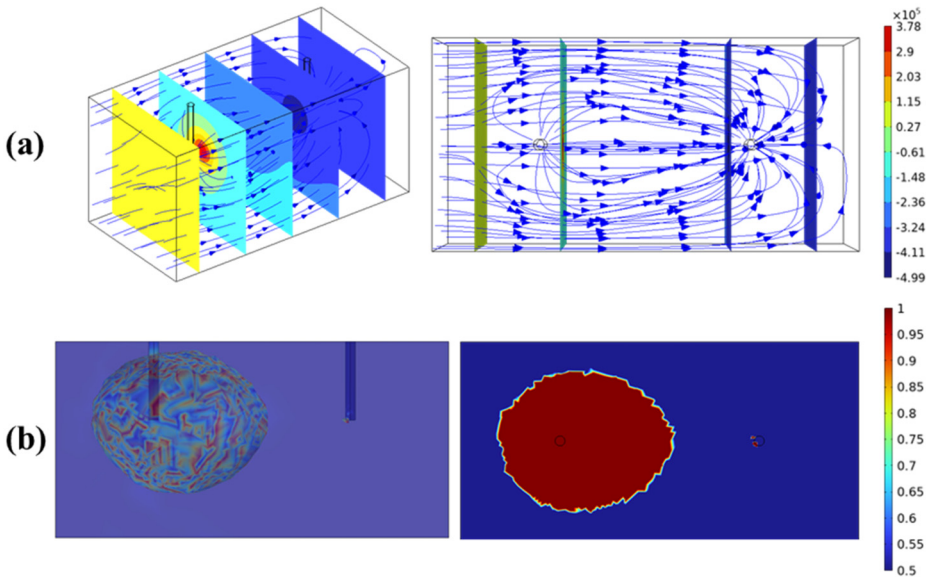

FIG. 11. Considering the diffusion seepage characteristics of slurry-water replacement aquifer sand layer grouting, pumping pressure 2 MPa. (a) Seepage pressure field variation and (b) slurry volume fraction variation.

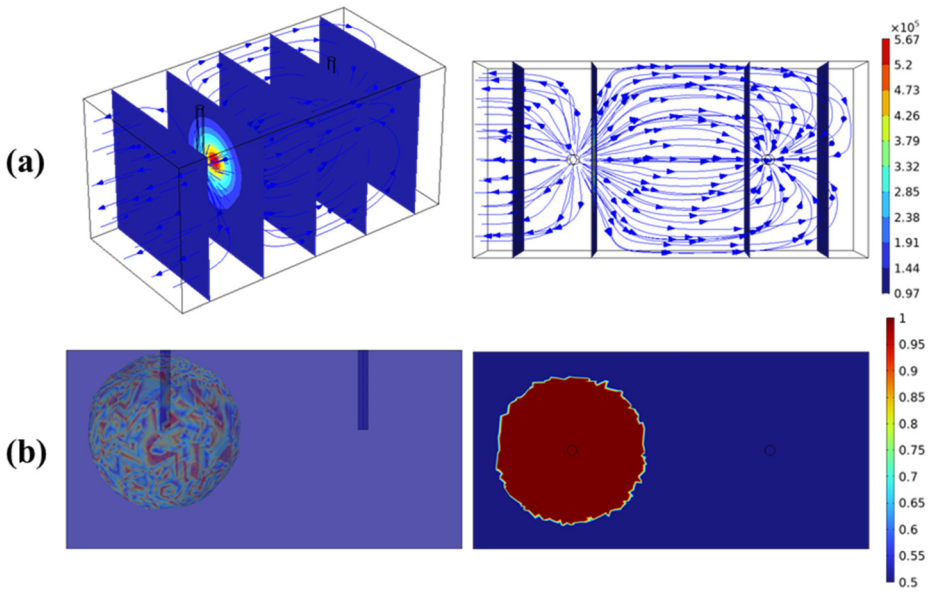

FIG. 12. Diffusion seepage characteristics of slurry-water replacement aquifer grouting without considering slurry-water replacement aquifer sand layer, pumping pressure 0 MPa. (a) Change of seepage pressure field and (b) change of slurry volume fraction.

layer and enhancing the stability of the sand layer. This achieves the purpose of transforming the water-bearing sand layer.

2. Horizontal spacing

Considering the slurry-water replacement effect, the model was established according to the above parameters, the grouting time was controlled at 1500 s, the water-cement ratio was set at 0.5, the grouting pressure was constant at 4 MPa, the pumping pressure was constant at 2 MPa, and only the interval between the grouting holes and the pumping holes was changed, to analyze the effect of the horizontal distance between the grouting holes and the drainage holes on the volume of the sand layer, and the results are shown in Figs. 13 and 14.

From Figs. 13 and 14, it can be observed that the spacing between drainage holes and grouting holes affects the grouting effectiveness. As the horizontal spacing between them increases, the maximum diffusion radius of the slurry enlarges, affecting the volume of the sand layer, showing a positive correlation. When the horizontal spacing is 0.5 m, the short distance between the two holes causes the slurry to quickly diffuse from the grouting hole to the drainage hole. The slurry saturation rapidly rises to the set range within a very short time. However, due to the spacing between the grouting hole and the drainage hole, as well as the drainage pressure, the slurry only diffuses around the drainage hole. In the numerical simulation process, refining the mesh around the two holes leads to excessive computation iterations, resulting in non-convergence situations. This also indicates that a too-small spacing may cause a smaller grouting diffusion range, a

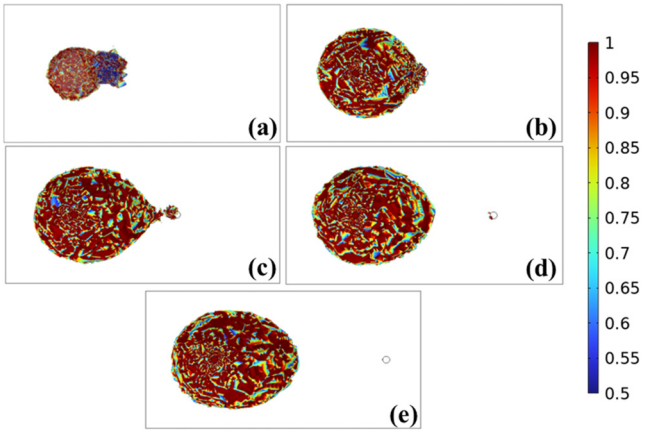

FIG. 13. Slurry diffusion pattern considering slurry-water displacement effect under different horizontal spacing: (a) Horizontal spacing 0.5 m (234 s, no convergence); (b) horizontal spacing 1.0 m; (c) horizontal spacing 1.5 m; (d) horizontal spacing 2.0 m; and (e) horizontal spacing of 2.5 m.

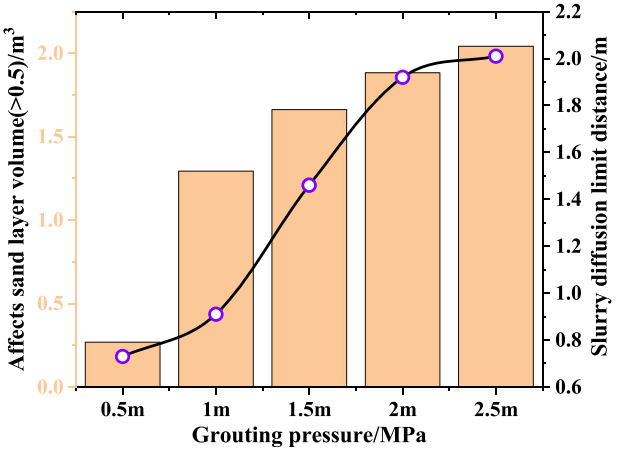

FIG. 14. Changes in volume and diffusion radius of impacted water-bearing sands with different horizontal spacing.

smaller volume of reinforced sand layer, increased grouting costs, and mining production costs. Moreover, during the drilling process, a too-small spacing may affect the integrity of adjacent holes, easily causing hole collapse and forming poorly sealed boreholes.

Over the same time period, with an increase in horizontal spacing, the diffusion distance of the slurry and its impact on the sand layer volume do not exhibit linear growth. When the horizontal spacing is 2 and 2.5 m, the growth rate continually slows down. It can be observed that with a larger horizontal interval, influenced by the tortuosity effect of the porous medium and the viscosity of the slurry, the resistance to slurry diffusion increases. Consequently, the diffusion range and the degree of displacement with pore water also slow down. Therefore, for the water-bearing sand layer and grouting slurry considered in this study, with a horizontal spacing of 2 m, the maximum diffusion radius is 1.92 m, impacting the sand layer volume by 1.88 m^3. When the horizontal spacing is 2.5 m, the maximum diffusion radius is 2.01 m, impacting the sand layer volume by 2.04 m^3. With an increase in horizontal spacing of 0.5 m, the diffusion radius only grows by 4.5%, and the impact on the sand layer volume only increases by 7.8%. Hence, considering the studied water-bearing sand layer and slurry, a horizontal spacing of 2 m between the two holes is more appropriate. Other geological conditions and slurry characteristics can be determined based on the research content.

3. Grouting pressure

Considering the pulp-water replacement effect, the model was established according to the above parameters, the grouting time was controlled at 1500 s, the water-cement ratio was set at 0.5, the interval between the grouting holes and the drainage holes was 2 m, the pumping pressure was constant at 2 MPa, and only the grouting pressure was changed, to analyze the effect of different grouting pressures on the maximum radius of spread of the slurry and the influence on the volume of the water-bearing sand layer, and the results were shown in Figs. 15 and 16.

From Fig. 15, it can be observed that under constant drainage pressure, the slurry diffusion radius is positively correlated with the grouting pressure. As the grouting pressure increases, the slurry continuously expands outward in a spherical shape, and the maximum diffusion radius gradually increases, expanding the solidification range volume of the surrounding loose sand layer. This is because the increased grouting pressure leads to a continuous expansion of the internal pressure difference within the porous medium. The influence range of the negative pressure zone increases, and with the constant drainage pressure, the volume of pore water steadily decreases, expanding the range of slurry filling into the pores of the sand layer.

From Fig. 16, it can be seen that the maximum slurry diffusion radius and the range affecting the sand layer exhibit non-linear growth with the linear increase in grouting pressure. The maximum diffusion radius shows varying degrees of attenuation. Within a certain range, higher grouting pressure leads to greater attenuation, and the impact on the sand layer volume slows to different extents. This is because in the loose water-bearing sand layer, the slurry encounters diffusion resistance due to the tortuosity effect of the sand layer and the viscosity of the slurry. This resistance slows down the extent of diffusion growth. Internal solid particles in the slurry adhere to the fine particles in the sand layer. Additionally, due to the gravity effect of the slurry, there is a certain degree of downward diffusion, resulting in a slowdown in the impact of the slurry on the volume of the water-bearing sand layer.

According to a study (Liu *et al.*, 2022), when the grouting pressure is too high, the slurry may create split cracks along the sand layer, leading to a limited extent of diffusion and easy accumulation of the slurry. Therefore, it is necessary to adjust the grouting pressure based on the geological conditions of the water-bearing sand layer on-site and the properties of the slurry.

4. Slurry viscosity

Considering the slurry-water replacement effect, the model was established according to the above parameters, the grouting time was controlled at 600 s, the interval between the grouting holes and the drainage holes was 2 m, the pumping pressure was constant at 2 MPa, and the grouting pressure was 4 MPa, and the water-cement ratio of the slurry was changed corresponding to the viscosity, and the effect of the time-variation of the slurry viscosity on the volume of the sand layer was analyzed, and the results were shown in Fig. 17.

From Fig. 17, it can be observed that, under the influence of viscosity over time, different viscosity power-law fluids exhibit spherical diffusion in the sand layer. The viscosity of the slurry affects its diffusion pattern in the sand layer. As the water-cement ratio of the slurry increases, resulting in lower viscosity, the inherent fluidity of the slurry increases, leading to a continuous expansion of the slurry's diffusion range in the sand layer and a sustained impact on the volume of the sand layer. When the water-cement ratio increases, the water content in the slurry rises, enhancing the inherent fluidity of the slurry. This decrease in dynamic viscosity allows the slurry to penetrate the pores of the sand layer more effectively, adhere to sand particles, and fill and reinforce the sand layer.

When considering the variable viscosity, the slurry diffusion changes over time. With increasing time, the viscosity also rises. In a limited time frame, taking a water-cement ratio of 0.7 as an example, the maximum diffusion radius of the slurry under effective grouting conditions is 0.63 m. However, when the slurry maintains a fixed viscosity unaffected by time, the maximum diffusion radius under effective grouting conditions is 0.98 m. Ignoring the time-dependent viscosity, the diffusion radius without considering viscosity variation is 1.55 times that of the maximum radius considering viscosity variation. As the grouting time continues to extend, the error will become increasingly significant. Therefore, the time-dependent nature of slurry viscosity is a crucial factor influencing slurry diffusion.

5. Porosity of aquifer sands

The porosity of the water-bearing sand layer corresponds to different deep-buried strata, and the porosity of the sand layer influences grouting efficiency. Considering the slurry-water displacement effect and based on the parameters mentioned above, a model is established. The grouting time is controlled at 1500 s, water-cement ratio is 0.7, the spacing between grouting holes and drainage holes is 2 m, constant pumping pressure is 2 MPa, and grouting pressure is 4 MPa. By varying the porosity of the sand layer, the impact of sand layer porosity on the maximum diffusion radius of the slurry and its influence on the volume of the water-bearing sand layer are analyzed. The results are shown in Figs. 18 and 19.

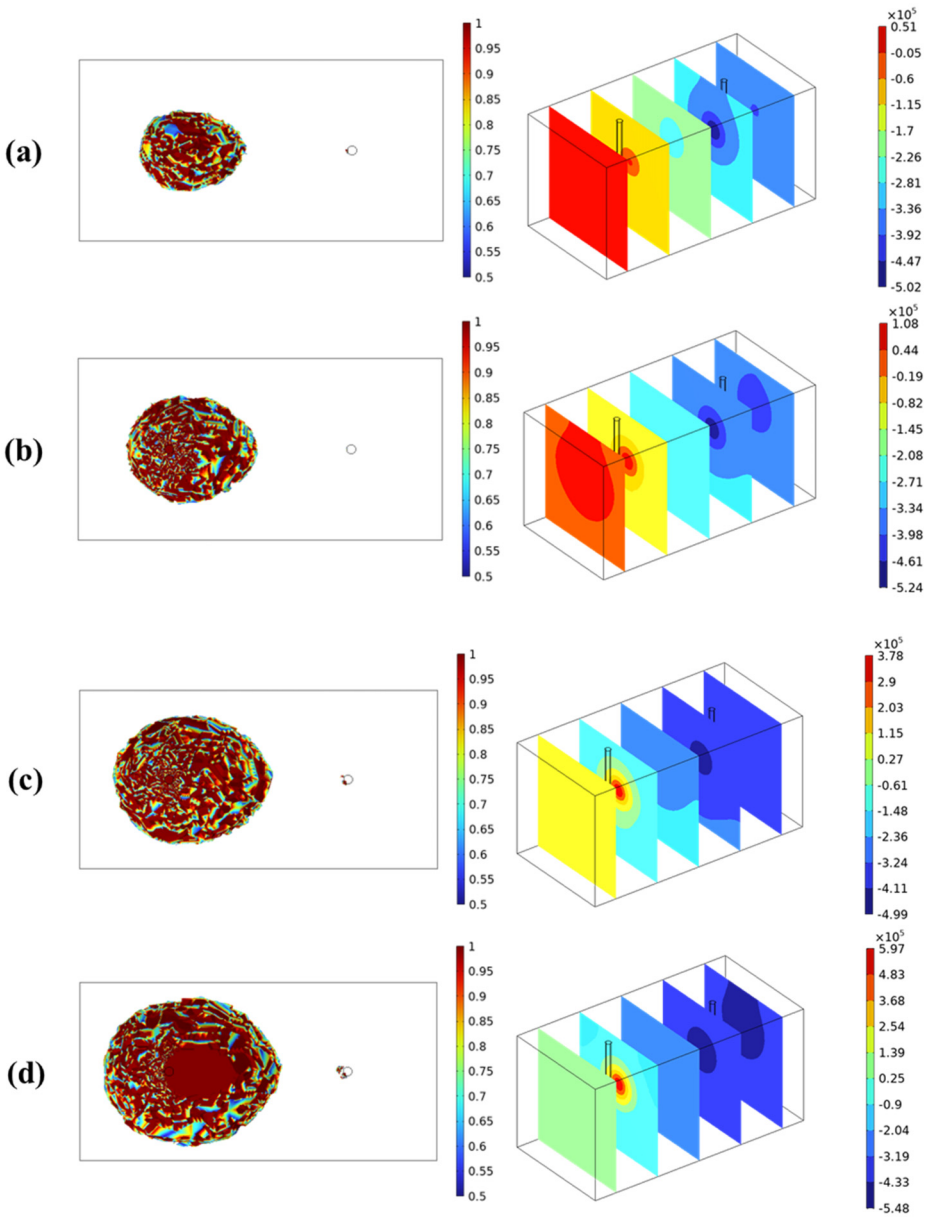

FIG. 15. Slurry diffusion pattern under different grouting pressures considering slurry-water replacement effect: (a) 1 MPa; (b) 2 MPa; (c) 4 MPa; and (d) 6 MPa.

According to Figs. 18 and 19, it can be observed that the porosity of the sand layer affects grouting efficiency. With the increase in sand layer porosity, the maximum diffusion radius of the slurry shows nearly linear growth. This is because the increased inter-particle voids in the sand layer result in reduced losses due to the tortuosity effect of the sand layer. As a result, the spreading degree of the slurry increases, and the diffusion range also enlarges. The efficiency of slurry displacing pore water improves. However, as the porosity of the sand layer continues to increase, the slurry can continuously inject into the sand layer within the porosity range of 0.36–0.43, leading to an increase in the volume of the reinforced sand layer. When the porosity increases to 0.5, although the increase in the maximum diffusion radius of the slurry is substantial, the rate at which the slurry affects the volume of the sand layer decreases. This is because in the early stages of slurry injection, the rapid diffusion rate is promoted by the increased porosity of the sand layer, driven by the grouting pressure and drainage pressure. The slurry-water displacement is more comprehensive. However, in the mid-to-late stages of grouting, due to the increasing resistance for the slurry to enter the pores of the sand layer caused by the slurry's viscosity and the bonding of slurry to sand particles during the early grouting process, the porosity decreases. This results in an increased resistance for the slurry to enter the pores of the sand layer, slowing down the increase in the volume of the reinforced sand layer.

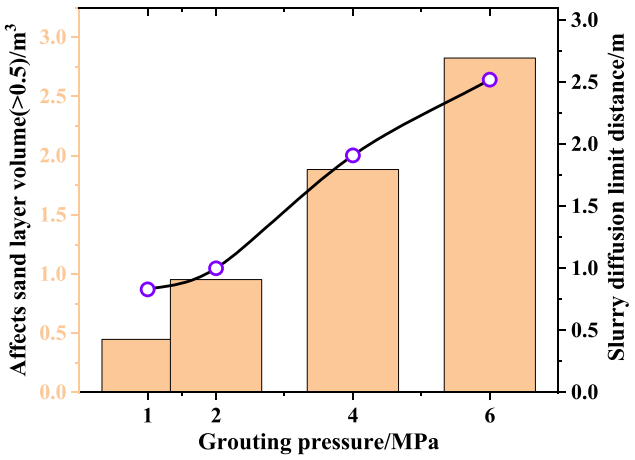

FIG. 16. Changes in volume and diffusion radius of water-bearing sand layer affected by different grouting pressures.

V. CONCLUSION

The study of slurry diffusion and reinforcement mechanisms in water-bearing sand layers during coal mining, which are prone to water inrush and sand collapse, is of great significance for mine safety production. This research not only provides valuable insights into the diffusion patterns of slurry in porous media, but also serves as a guideline for underground reconstruction of water-bearing loose sand layers. The conclusions drawn are as follows:

(1) This study first proposed the concept of slurry-water displacement, considering the tortuosity effect of porous media. Based on Darcy's law and the mass conservation equation, a power-law fluid penetration grouting spherical diffusion mechanism that takes into account the tortuosity effect and slurry-water displacement effect in loose water-bearing sand layers was established, and the applicable range of the formula was given.
(2) A grouting diffusion test platform for water-bearing sand layers was set up to analyze the differences between theoretical results and laboratory test results with or without slurry-water

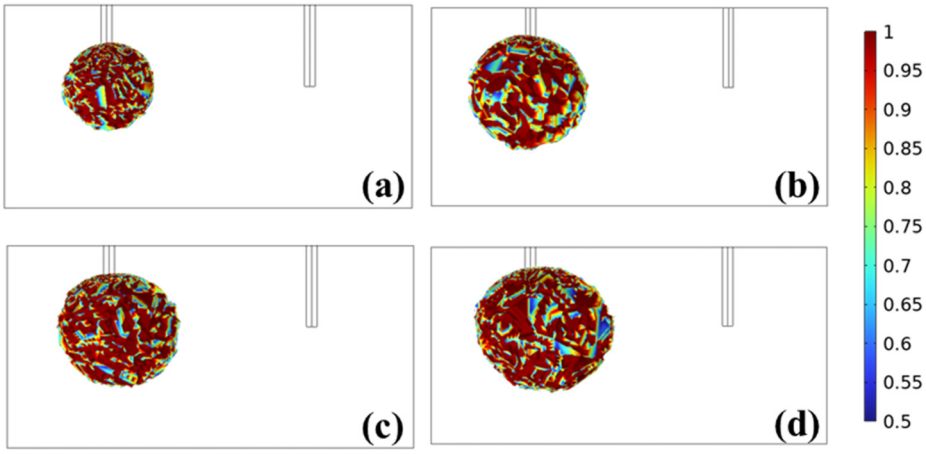

FIG. 17. Effect of time-varying slurry viscosity on diffusion range for different water-cement ratios: (a) Water-cement ratio of 0.5; (b) water-cement ratio of 0.6; (c) water-cement ratio of 0.7; and (d) without considering the time-varying viscosity of the slurry.

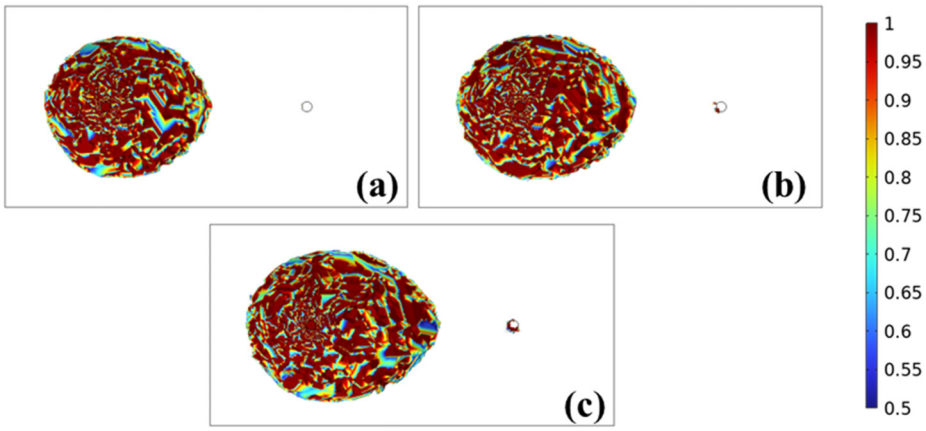

FIG. 18. Slurry diffusion pattern under consideration of slurry-water displacement effect in different sand layer porosity: (a) Porosity of 0.36; (b) porosity of 0.43; and (c) porosity of 0.5.

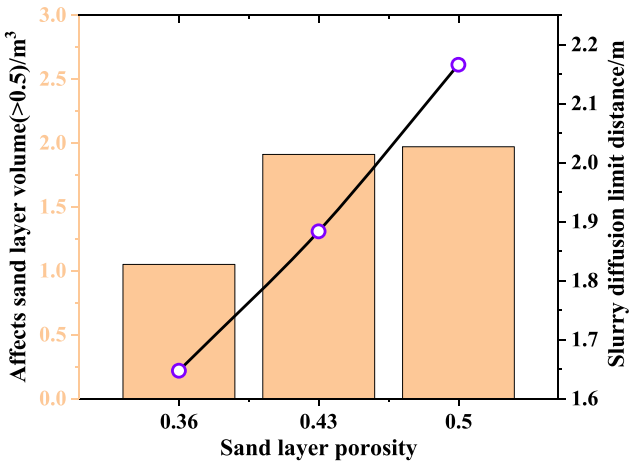

FIG. 19. Changes in volume and diffusion radius of impacted water-bearing sands with different sand porosities.

displacement, with or without the tortuosity effect of porous media, and the superposition of both effects. The verification shows that the tortuosity effect of porous media affects the diffusion of slurry, and the spherical diffusion equation of slurry considering the tortuosity effect of porous media and slurry-water displacement effect has an error range of less than 20% compared with field tests, indicating the rationality of the theoretical model.

(3) Utilizing the secondary development of COMSOL numerical simulation software, a three-dimensional numerical model of power-law fluid grouting spherical diffusion considering the tortuosity effect of porous media and slurry-water displacement effect was established. It initially demonstrates that the slurry diffusion effect under the consideration of slurry-water displacement is good and has a guiding nature, which can more effectively reinforce the water-bearing sand layer.

(4) Through numerical simulation, the influence of slurry-water hole horizontal spacing, slurry viscosity, grouting pressure, and sand layer porosity on the slurry diffusion radius and reinforced sand layer volume was analyzed. It was concluded that the slurry-water hole horizontal spacing and grouting pressure need to be controlled within a reasonable range and should not be blindly increased, determined according to actual geological conditions. Compared with previous grouting techniques and processes, slurry-water displacement grouting technology can solve problems such as small grouting diffusion range and poor grouting effect in high-pressure water-bearing sand layers to a certain extent, providing safety guarantees for coal production.

The focus of this study is on the diffusion mechanism of slurry in water-bearing sand layers, without considering the mutual influence of slurry on sand particles. Future research can focus on the following aspects: (1) the critical point of slurry-sand migration, including the interaction of slurry-sand migration under different particle size gradations; (2) the effect inspection of slurry-sand mixtures after grouting, including the bearing strength and resistance to hydrodynamic erosion of the mortar mixture; (3) the layout of drainage pipes, considering not only the same horizontal level, but also different aperture sizes and different strata, which also affect the efficiency of slurry-water displacement. (4) Currently, only numerical simulation methods are used for analysis, and further verification of the research's rationality through field tests is still needed.

Based on the current research foundation, the above issues can be further explored to improve the theory and technical system of grouting reconstruction of water-bearing sand layers, providing guidance value for practical applications in the field.

ACKNOWLEDGMENTS

The project was supported by the National Natural Science Foundation of China (No. 51774199) and Natural Science Foundation of Shandong Province (No. ZR2023ME066).

AUTHOR DECLARATIONS

Conflict of Interest

The authors have no conflicts to disclose.

Author Contributions

Xianxiang Zhu: Data curation (equal); Methodology (equal); Writing – original draft (equal). **Qi Zhang:** Data curation (equal); Methodology (lead); Writing – review & editing (equal). **Wenquan Zhang:** Methodology (equal); Resources (lead); Supervision (lead). **Lei Jin:** Data curation (lead). **Zixu Li:** Software (equal).

DATA AVAILABILITY

The data that support the findings of this study are available from the corresponding author upon reasonable request.

REFERENCES

Civan, F., "Effective correlation of apparent gas permeability in tight porous media," Transp. Porous Media **82**(2), 375–384 (2010).

Dong, H. L., Wang, S. F., and Li, X. P., "Drainage-induced displacement grouting technology in saturated confined water sand layers," Tunnel Constr. **42**(2), 215 (2022).

Fang, J., Li, Q. S., Du, W. F., and Cao, Z. G., "Water disaster control in overlying thick loose layer on bedrock in Shendong coal mining area," Coal Geol. Explor. **44**(4), 94–97 (2016).

Fraccica, A., Spagnoli, G., Romero, E., Arroyo, M., and Gómez, R., "Permeation grouting of silt-sand mixtures," Transp. Geotech. **35**, 100800 (2022).

GB/T50123, "Standard of geotechnical test method," Standard No. GB/T 50123-2019 (China National Standards, China, 2019).

Guo, T. T., Zhang, Z. W., Yang, Z. Q. *et al.*, "Penetration grouting mechanism of time-dependent power-law fluid for reinforcing loose gravel soil," Minerals **11**(12), 1391 (2021).

Han, C. H., Wei, J. C., Zhang, W. J. *et al.*, "Quantitative permeation grouting in sand layer with consideration of grout properties and medium characteristics," Constr. Build. Mater. **327**, 126947 (2022).

Hou, D. F., Li, D. H., Xu, G. S., and Zhang, Y. B., "Superposition model for analyzing the dynamic ground subsidence in mining area of thick loose layer," Int. J. Min. Sci. Technol. **28**(4), 663–668 (2018).

Huang, F., Lyu, J. G., Gao, H., and Wang, G. H., "Modified Maag's spherical diffusion model of vacuum penetration grouting," Math. Probl. Eng. **2018**(1758651), 1–7.

Kalore, S. A. and Babu, G. L. S., "Hydraulic conductivity requirement of granular and geotextile filter for internally stable soils," Geotext. Geomembr. **50**(3), 510–520 (2020).

Kong, X. Y., *Advanced Mechanics of Fluid in Porous Media* (University of Science and Technology of China Press, Beijing, 1999).
Li, B., Zhang, W. Q., and Ma, L., "Influencing factors and prediction of mine water inrush disaster under thick unconsolidated lavers and thin bedrock," J. Shandong Univ. Sci. Technol. (Nat. Sci.) **36**(06), 39–46 (2017).
Li, H. J., Li, J. H., Li, L., Xu, H., and Wei, J. J., "Prevention of water and sand inrush during mining of extremely thick coal seams under unconsolidated Cenozoic alluvium," Bull. Eng. Geol. Environ. **79**(6), 3271–3283 (2020).
Liu, H., Li, Y., Su, L. J. *et al.*, "Surface deformation law of mining under thick loose layer and thin bedrock: Taking the southern Shandong mining area as an example," Coal Sci. Technol. **51**(9), 11–23 (2023).
Liu, J., Zhang, L., Xue, H. S., You, T., and Wu, Y. Q., "Technique of grouting in silty-fine sand with abundant water: Practice in Beijing," Geomech. Eng. **29**(4), 463–470 (2022).
Ma, J. B., Yin, D. W., Jiang, N., Wang, S., and Yao, D. H., "Application of a superposition model to evaluate surface asymmetric settlement in a mining area with thick bedrock and thin loose layer," J. Clean. Prod. **314**, 128075 (2021).
Mollamahmutoglu, M. and Yilmaz, Y., "Engineering properties of medium-to-fine sands injected with microfine cement grout," Mar. Georesour. Geotechnol. **29**(2), 95–109 (2011).
Pantokratoras, A., "Steady flow of a power-law non-Newtonian fluid across an unconfined square cylinder," J. Appl. Mech. Tech. Phys. **57**(2), 264–274 (2016).
Peng, S. L., Cheng, H., Yao, Z. S., Rong, C. X., Cai, H. B., and Zhang, L. L., "Study on prediction and characteristics of surface subsidence in mining when the bottom aquifer of thick loose layer directly covers thin bedrock," J. China Coal Soc. **47**(12), 4417–4430 (2022).
Song, M. L., Wang, J. L., and Zhao, J. J., "Coal endowment, resource curse, and high coal-consuming industries location: Analysis based on large-scale data," Resour. Conserv. Recycl. **129**, 333–344 (2018).
Wang, C. J., Diao, Y. L., Guo, C. C., Li, P., Du, X. M., and Pan, Y. H., "Two-stage column–hemispherical penetration diffusion model considering porosity tortuosity and time-dependent viscosity behavior," Acta Geotech. **18**(5), 2661–2680 (2023).
Wang, Z. Y., Lian, H. J., Liang, W. G. *et al.*, "Experimental study on the fracture process zones and fracture characteristics of coal and rocks in coal beds," Rock Mech. Rock Eng. **57**(2), 1375–1393 (2023).
Xie, B., Chen, H., Wang, X. S *et al.*, "Theoretical Research on Diffusion Radius of Cement-Based Materials Considering the Pore Characteristics of Porous Media Materials," Materials **15**(21), 7763 (2022).
Yang, X. Z., Lei, J. S., Xia, L. N., and Wang, X. H., "Study on grouting diffusion radius of exponential fluids," Rock Soil Mech. **26**(11), 112–115 (2005).
Yang, Z. Q., Lu, J., Wang, Y. *et al.*, "Column penetration grouting mechanism for power-law fluids considering tortuosity effect of porous media," Chin. J. Rock Mech. Eng. **40**(02), 410–418 (2021).
Ye, F., Qin, N., Han, X., Liang, X., Gao, X., and Ying, K. C., "Displacement infiltration diffusion model of power-law grout as backfill grouting of a shield tunnel," Eur. J. Environ. Civ. Eng. **26**(5), 1820–1833 (2020).
Ye, F., Yang, T., Mao, J. H., Qin, X. Z., and Zhao, R. L., "Half-spherical surface diffusion model of shield tunnel back-fill grouting based on infiltration effect," Tunneling Underground Space Technol. **83**, 274–281 (2019).
Yu, Z. B., Zhu, S. Y., Wu, Y., and Yu, H. T., "Study on the structural characteristics of the overburden under thick loose layer and thin-bed rock for safety of mining coal seam," Environ. Earth Sci. **79**(1), 9 (2020).
Zeng, X. X., *Mud Rheology and Viscosity Measurement* (Geological Society of Hunan, Changsha, 1981).
Zhang, G. B., "Study on the model of water and sand inrush and its mechanism caused by mining under alluvium," Ph.D. dissertation (Shandong University of Science and Technology, 2017).
Zhang, Q., Yin, Z. Y., and Yan, X., "Anisotropic continuum framework of coupled gas flow - adsorption - deformation in sedimentary rocks," Int. J. Numer. Anal. Methods Geomech. **48**, 1018–1045 (2024a).
Zhang, Q., Yin, Z. Y., and Yan, X., "Material constants of anisotropic poroelasticity and its impacts on shale gas production," Energy Fuels **37**, 18722–18734 (2023b).
Zhang, S., Peng, R., Ye, X. Y., Xie, L. B., Lei, Y., and Li, Y., "Experimental evaluation of the performance of a geotextile for a pressure-grouted soil nail," Geotext. Geomembr. **50**(3), 498–509 (2022).
Zhang, W. Q., Lei, Y., Shao, J. L., Wu, X. A., Li, S., and Ma, C. Q., "Simulation of the activation of mining faults and grouting reinforcement under thick loose layer and thin bedrock," Sci. Rep. **12**(1), 17049 (2022).
Zhang, W. Q., Zhu, X. X., Lv, W. M., Wang, Y. J., and Li, S., "Research on the preparation and diffusion characteristics of coal seam bottom fracture grouting material based on solid waste synergy," J. Clean. Prod. **422**, 138557 (2023).
Zhu, X. X., Zhang, W. Q., Wang, Y. J., Lv, W. M., and Ma, C. Q., "Diffusion mechanism of solid waste product utilization pulping and fracture network grouting," Constr. Build. Mater. **408**, 133571 (2023).